Figure S1

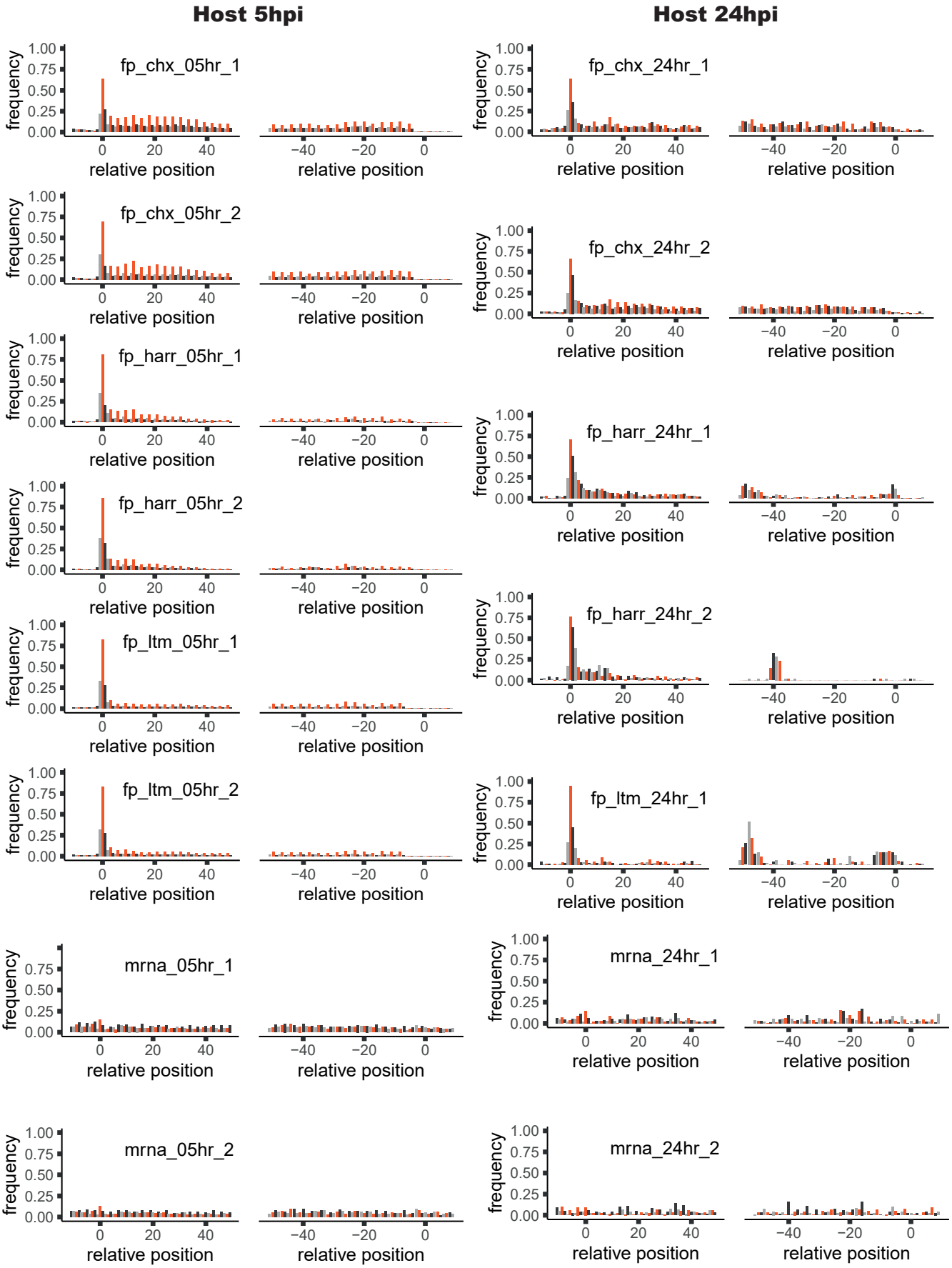

Figure S1. Footprint profiles of cellular coding genes from SARS-CoV-2 infected cells
Metagene analysis of read densities at the 5′ and the 3′ regions of cellular protein coding genes as measured by the different ribosome profiling approaches and RNA-seq at 5hpi and 24hpi, from two biological replicates (expect for one LTM replicate from 24hpi for which there were not enough reads). The X axis shows the nucleotide position relative to the start or the stop codons. The ribosome densities are shown with different colors indicating the three frames relative to the main ORF (red, frame 0; black, frame +1; grey, frame +2).

Figure S2

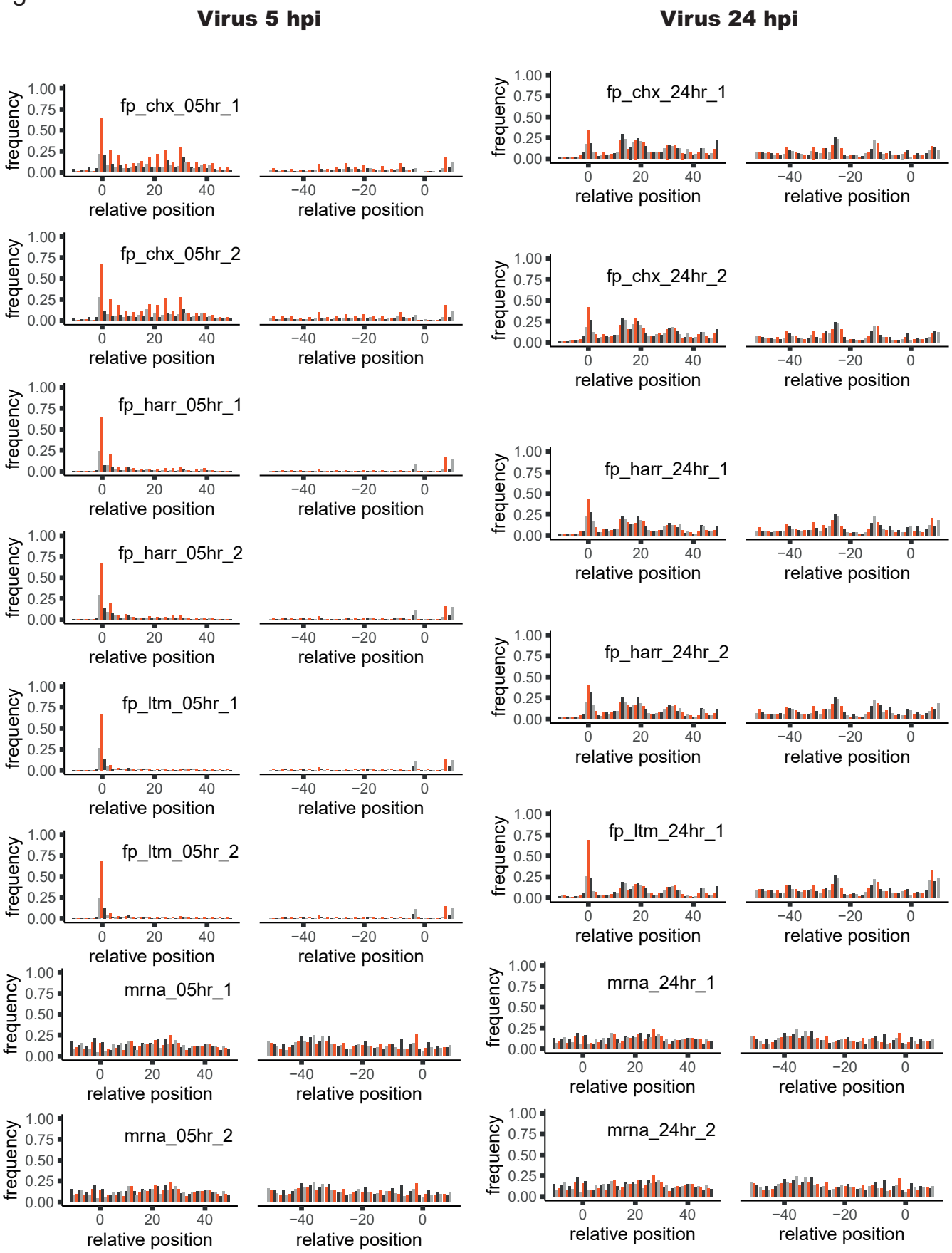

Figure S2. Footprint profiles of viral coding genes from SARS-CoV-2 infected cells
Metagene analysis of read densities at the 5′ and the 3′ regions of viral protein coding genes as measured by the different ribosome profiling approaches and RNA-seq at 5hpi and 24hpi, from two biological replicates (expect for one LTM replicate from 24hpi for which there were not enough reads). The X axis shows the nucleotide position relative to the start or the stop codons. The ribosome densities are shown with different colors indicating the three frames relative to the main ORF (red, frame 0; black, frame +1; grey, frame +2).

Figure S3

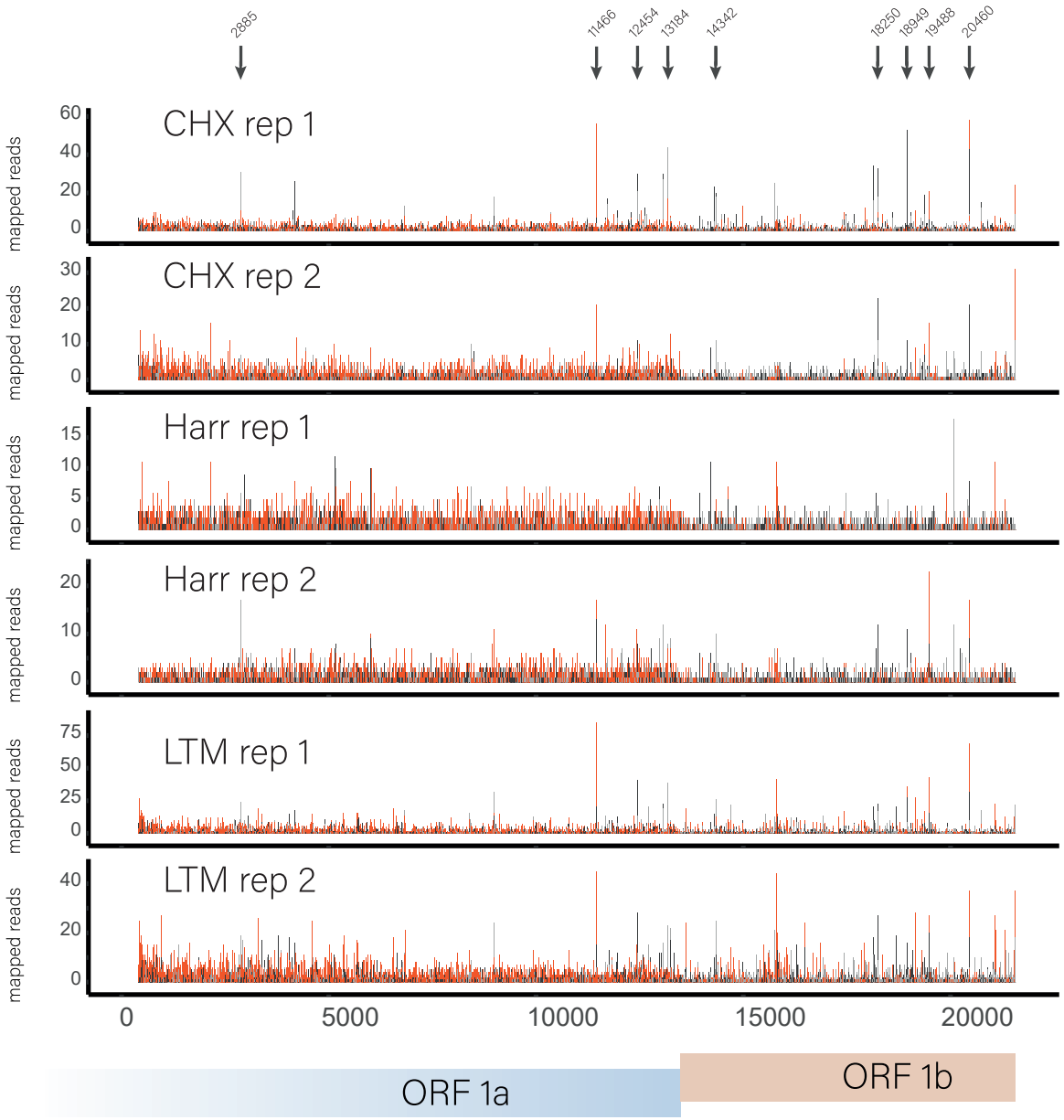

Figure S3. Ribosome densities reveal potential ribosome pausing sites within ORF1a and ORF1b

Ribosome densities are presented for ORF1a and ORF1b at 5hpi from two biological replicates. Different colors indicating the three phases relative to the translated frame (red, frame 0; black, frame +1; grey, frame +2). Black arrows mark potential ribosome pausing sites and their genomic positions.

Figure S4

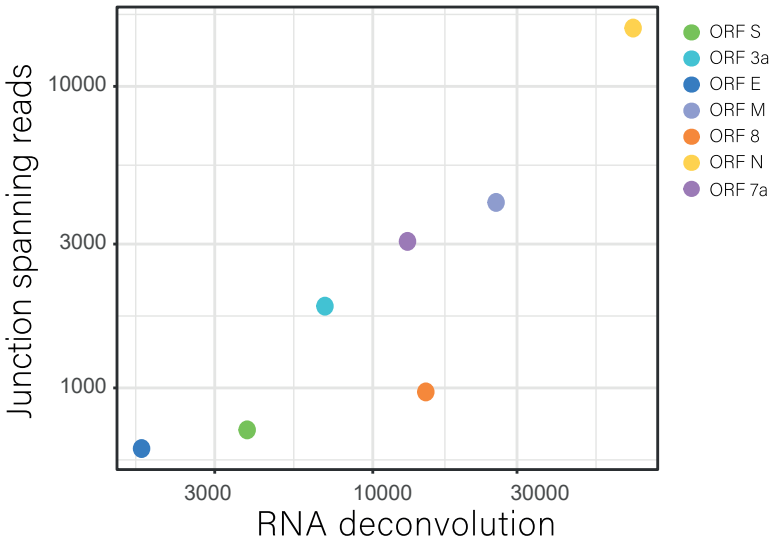

Figure S4. Correlation between two approaches for calculating abundance of subgenomic RNAs

Measurement of subgenomic RNA abundance using deconvolution of RNA densities versus using relative abundance of RNA reads spanning leader-body junctions, for seven canonical viral ORFs.

Figure S5

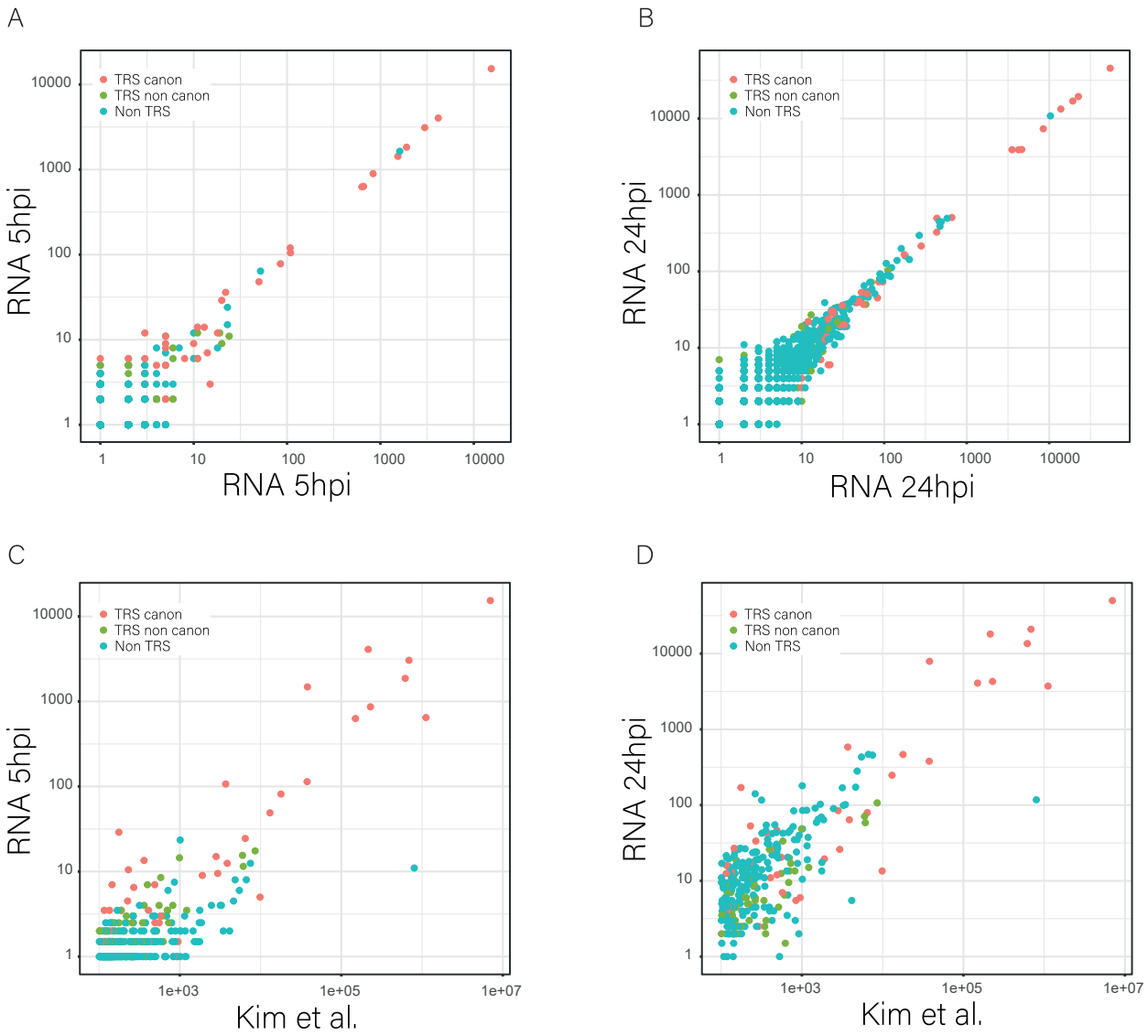

Figure S5. Correlation between junction-spanning RNA-seq reads from different samples
Scatter plots presenting the abundance of junction-spanning RNA-seq reads from two biological replicates from (A) 5hpi and (B) 24hpi. Scatter plots presenting the average abundance of junction-spanning RNA-seq reads from (C) 5hpi or (D) 24hpi versus data from Kim et al. Viral reads that span canonical leader dependent junctions are marked in red, non-canonical leader dependent junctions are marked in green and non-canonical leader independent junctions are marked in cyan.

Figure S6 - page 1

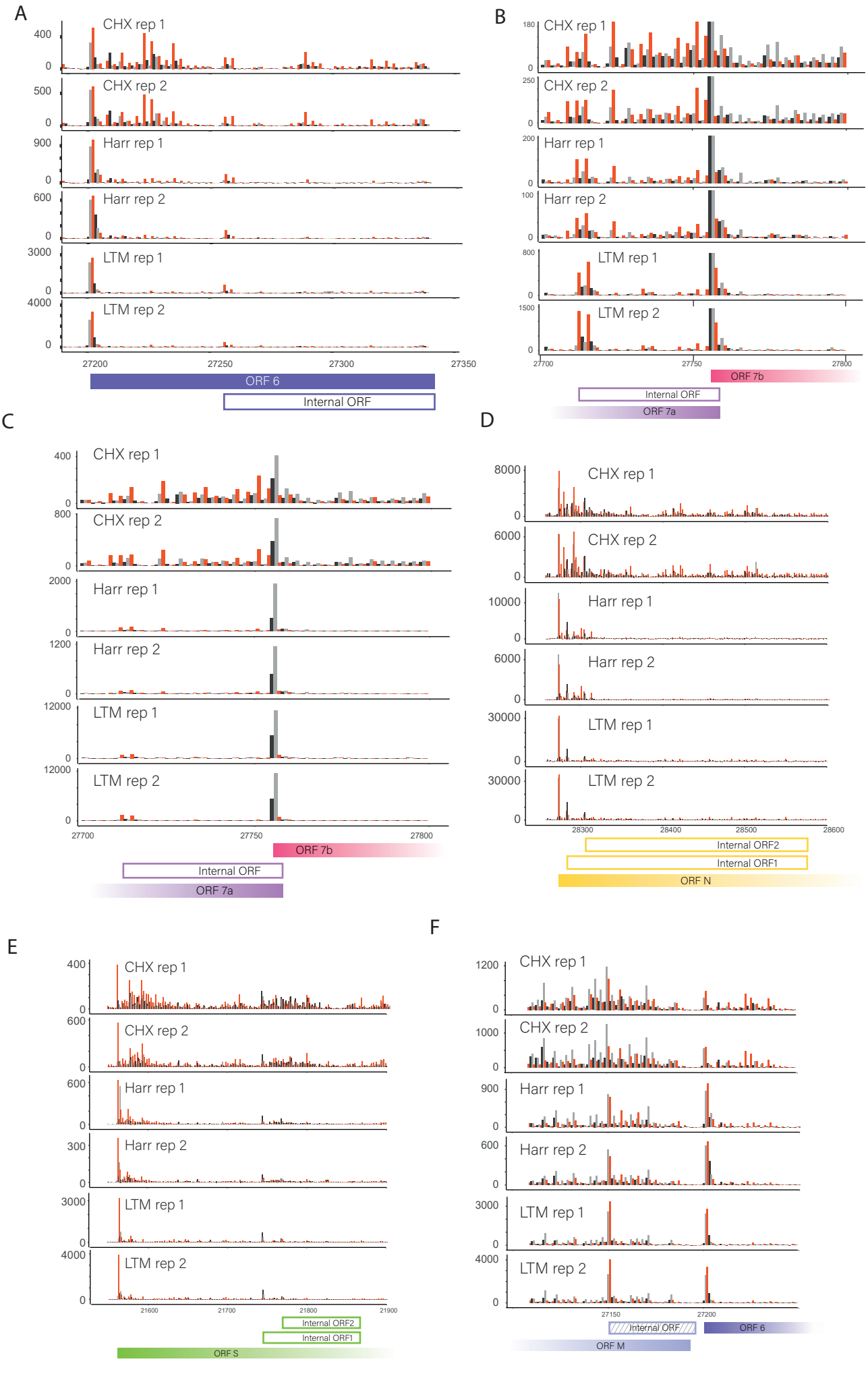

Figure S6 - page 2

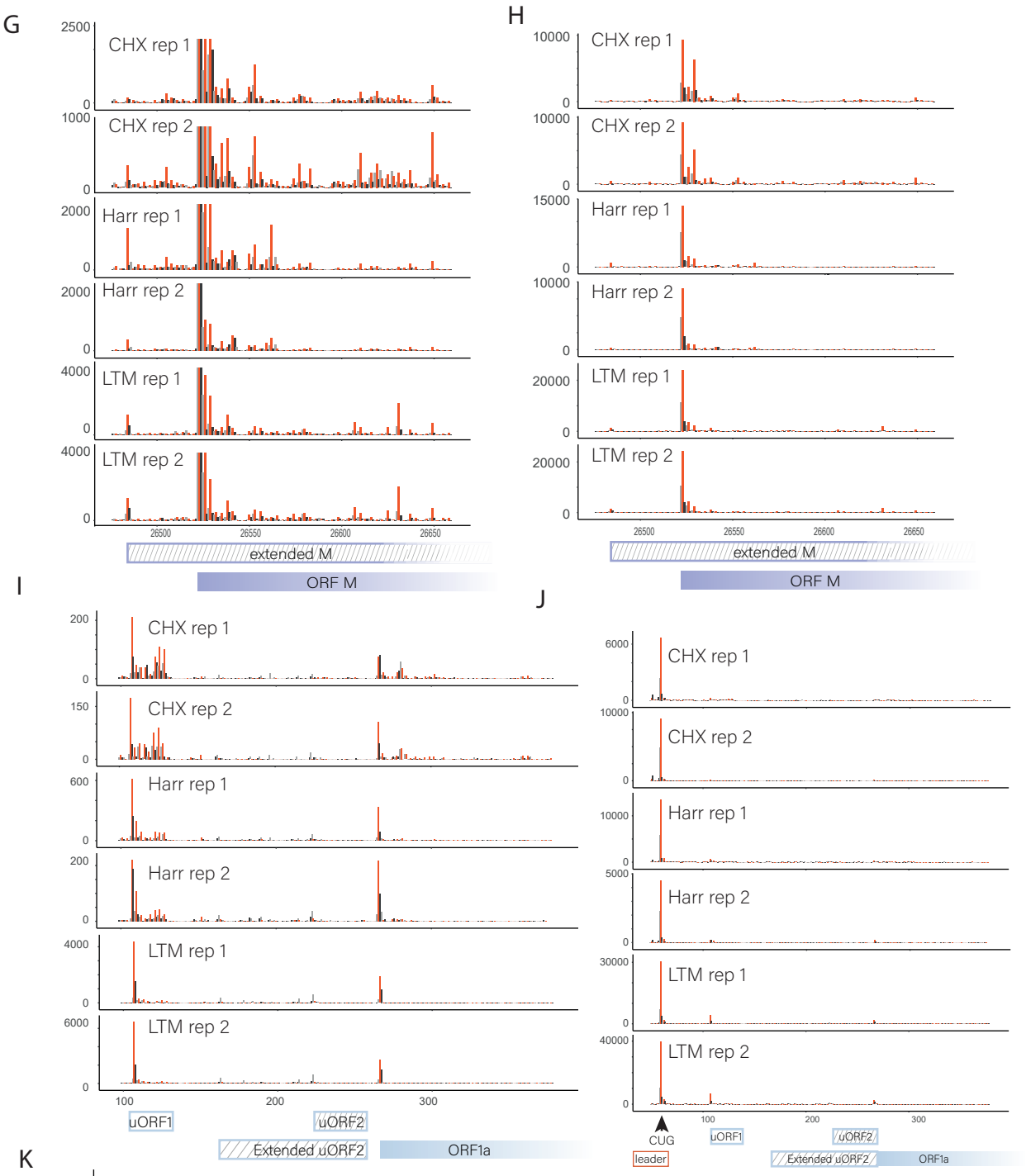

Figure S6. Ribosome densities reveal novel viral coding regions (A-K) Ribosome density profiles of CHX, Harr and LTM samples from both replicates at 5 hpi are presented. Densities are shown with different colors indicating the three frames relative to the main ORF in each figure (red, frame 0; black, frame +1; grey, frame +2). Rectangles indicate the canonical and novel ORFs and ORFs starting in near cognate are labeled with stripes. (A) In frame internal initiation within ORF6 generating truncated product (as shown in Figure 3A). (B and C) In frame internal initiation within ORF7a (as shown in Figure 3B), (B) scale is adapted to present the internal ORF initiation (C) full scale presenting ORF7b initiation in true scale. (D) Out of frame internal initiation within ORF-N (as shown in Figure 3C). (E) Out of frame internal initiation within ORF-S (as shown in Figure 3D). (F) Out of frame internal initiation within ORF-M (as shown in Figure 3E). (G-H) an extended version of ORF-M (as shown in Figure 3F) (G) scale is adapted to present the extended ORF (H) full scale presenting the dominance of the main initiation, (I) two uORFs embedded in ORF1ab 5'UTR (as shown in Figure 3G) (J) non canonical CUG initiation upstream of the TRS leader (as shown in Figure 3H) (K) uORF that overlap ORF10 initiation and in frame internal initiation generating truncated ORF10 product (as shown in Figure 3I).

Figure S7

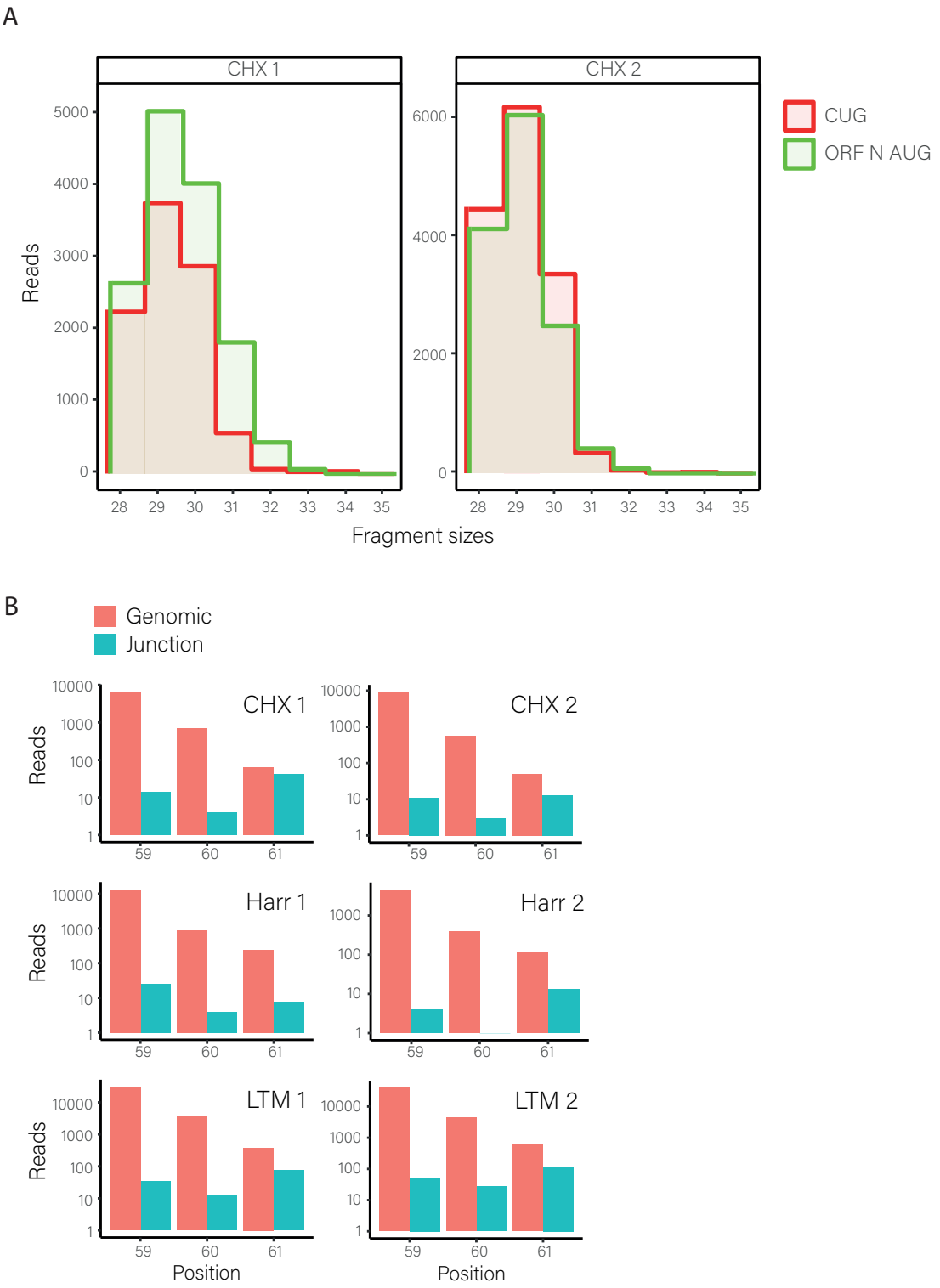

Figure S7. The CUG initiation stem from genomic RNA
(A) Comparison of the ribosome footprint read length distributions of reads that align to the CUG (red) and reads that align to ORF-N AUG (green). (B) The number of ribosome profiling reads from 5 hpi that their P-site was mapped to positions 59, 60 and 61 and align to the genome (orange) or to leader-body junctions (cyan).

Figure S8

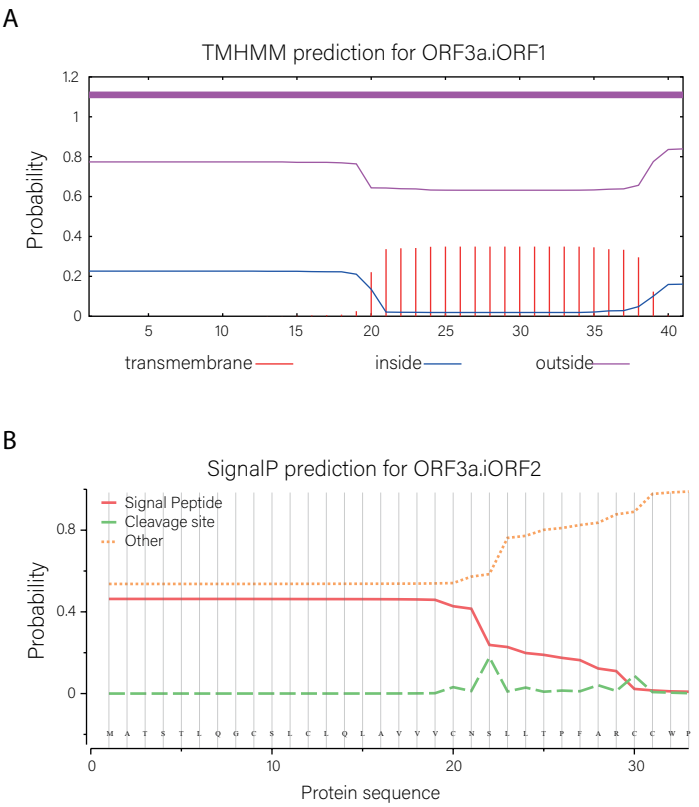

Figure S8. Transmembrane and signal peptide predictions
(A) Transmembrane region predicted in 3a.iORF1 using TMHMM 2.0
(B) signal peptide prediction in 3a.iORF2 as predicted using SignalP 5.0

Figure S9

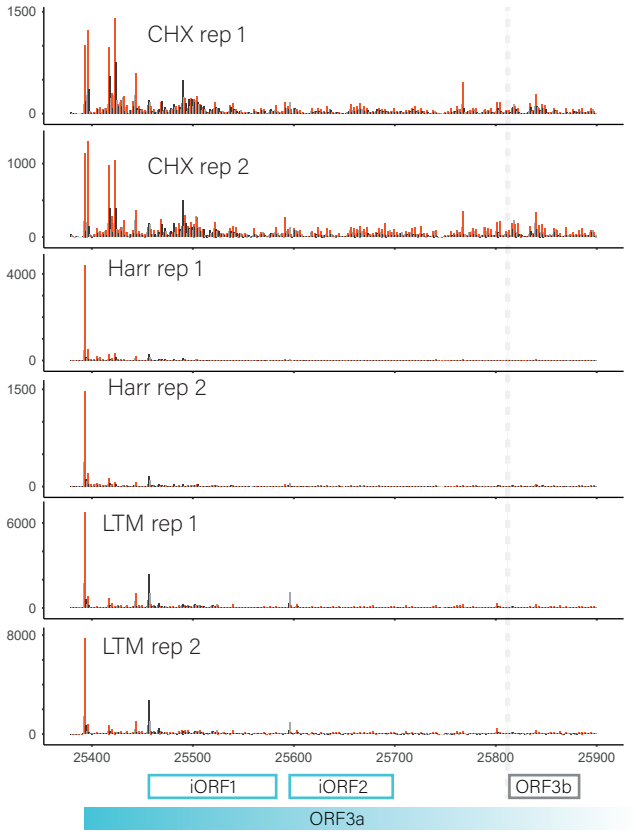

Figure S9 internal ORFs encoded within ORF3a
Ribosome density profiles of CHX, Harr and LTM samples from both replicates at 5 hpi are presented. Densities are shown with different colors indicating the three frames relative to the main ORF in each figure (red, frame 0; black, frame +1; grey, frame +2). Rectangles indicate the canonical and novel ORFs. ORF3b is marked based on the homology to SARS-CoV.

Figure S10

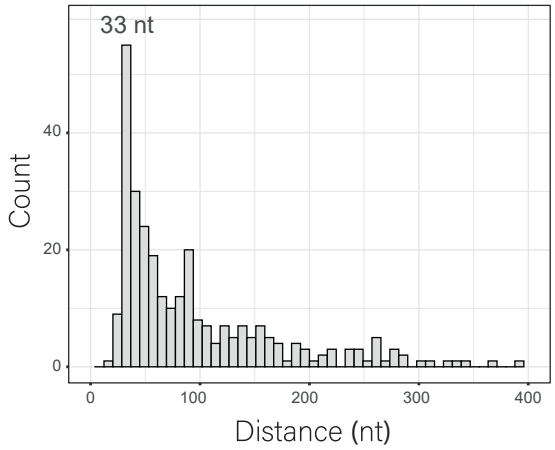

Figure S10. Distance distribution of footprint peaks at 24 hpi
Distribution of distances between adjacent prominent ribo-seq peaks from 24 hpi.